EUROPEAN ORGANISATION FOR NUCLEAR RESEARCH

CERN/ISRC/81-19
September 1,1981

LETTER OF INTENT TO THE ISRC

STUDY OF LIGHT ION INTERACTIONS WITH THE SFM DETECTOR

W.Bell[1],K.Braune[2],G.Claesson[3],K.Doroba[9],D.Drijard[1],
M.A.Faessler[2],H.G.Fischer[1],H.Frehse[1],R.W.Frey[4],S.Garpman[3],
W.Geist[5],R.Gokieli[10],C.R.Gruhn[7],P.C.Gugelot[6],P.Hanke[1],
M.Heiden[5],P.G.Innocenti[1],T.J.Ketel[2],E.E.Kluge[5],G.Mornacchi[1],
T.Nakada[5],I.Otterlund[3],H.Pugh[7],A.Putzer[5],K.Rauschnabel[8],
L.Schroeder[7],R.Sosnowski[10],E.Stenlund[3],T.J.M.Symons[7],
M.Szczecowski[8],R.Szwed[2],O.Ullaland[1]

CERN-DORTMUND-HEIDELBERG-LBL-LUND-WARSAW COLLABORATION

1) CERN, Geneva, Switzerland
2) Max Planck Institut für Kernphysik, Heidelberg, Germany
3) Division of Cosmic and Subatomic Physics, Univ. of Lund, Sweden
4) Physikalisches Institut der Universität Heidelberg, Germany
5) Institut für Hochenergiephysik der Universität Heidelberg, Germany
6) Physics Department, University of Virginia, Charlottesville, VA, USA
7) Nuclear Science Division, LBL, Univ. of California, Berkeley, CA, USA
8) Physikalisches Institut der Universität Dortmund, Germany
9) University of Warsaw, Poland
10) Institute for Nuclear Research Warsaw, Poland

1. INTRODUCTION

We wish to inform the ISRC about our intention to ask for further running time with αα and αp, and possibly also with dd and dp beams in the second half of 1982.

The analysis of all data taken in the week of running with α particles in July/August 1980 is not completed yet, but has already progressed far enough to reveal several reasons to continue with more data taking [1,2,5,6,13]. On one hand, more luminosity is needed, simply to improve the statistics of part of the data. On the other hand we plan to extend the measurements with some new improvements to the detector. Finally we would still like to have a run at lower energy as requested in the original proposal and to have, for comparisons, short runs with dd and dp beams. In the following, these reasons are explained in some more detail.

2. ELASTIC αp AND αα SCATTERING

The differential cross sections measured by R418 are shown in fig.1 and compared with the ones measured by R210/211[1,2] and with data taken at lower energies[3,4].

The lower cut in t for the SFM data (taken at beam energies of 31.5xQ GeV) is around 0.2 $(GeV/c)^2$, due to the mimimum detectable angle of 7 mrad (t_{min}= $(.007x63\ GeV/c)^2$).

With a beam energy of 22xQ GeV the t-cut will be at t_{min}= 0.1 $(GeV/c)^2$. Thus a measurement of dσ/dt(αp) around the first diffraction minimum (at 0.14 GeV/c^2) and of dσ/dt(αα) right above the first minimum is possible. This energy would also connect to the FNAL measurement of elastic αp scattering[4].

At the highest energy, 31xQ GeV, we wish to extend the measurements to higher t values and to improve the statistics in the range already studied.

The preliminary data for the elastic differential cross sections of $\alpha\alpha$ and αp in the ISR have already stimulated several theoreticians to do calculations. Although the results of these calculations are not known to us yet, it is already clear that more and better data will be welcome.

3. LARGE p_t PARTICLE PRODUCTION

The yield of charged particles with large p_t in $\alpha\alpha$ collisions relative to the yield in pp collisions at the same $\sqrt{s_{nn}}$ was found to be higher than 16 and to increase with p_t. (fig.2 and 3)[5,6]. --A factor $16=A^2$ is what one would naively expect for 4x4 independently interacting nucleon-pairs. Similar results were also obtained by two other experiments (R110 and R806) measuring π^0 production[7,8].

One of the motivations to perform the experiment with α particles in the ISR was to search for the origin of the 'anomalous nuclear enhancement' (ANE) previously found at FNAL for the production of large p_t charged hadrons in proton-nucleus interactions[9]. Thus in case of αp interactions the cross sections were expected to be 5 times higher than in pp interactions for p_t around 3 to 4 GeV/c, i.e. an enhancement of 20% was expected. The data (fig.3) do not prove such an enhancement but are compatible with it.

The search for the origin of the ANE has suffered so far from low statistics, see for instance the x_e distributions of away particles (fig. 4). If the ANE is caused by multiple semihard scattering of partons, one expects a steepening of the distributions at large x_e in $\alpha\alpha$ and αp interactions as compared to pp interactions. Multiple parton scattering was proposed as possible mechanism by several authors to explain the ANE[10]. However, at large x_e (say above .5) the statistics of the data is marginal. About a factor 10 more statistics is needed to obtain good sensitivity to differences in the interesting x_e region. This could be achieved in runs of similar length as the first.

In the first run two independent trigger regions at 45⁰ were used. In the mean time, trigger roads have been set up and are operating at 20⁰ and 10⁰ with respect to one beam and one of the trigger roads at 45⁰ has been kept. Thus a wider range of physics can be explored. In principle it is now possible to measure the inclusive production in αp collisions at 6 different angles in two runs, where the beams are reversed once, exploiting the fact that the c.m. moves with a rapidity y=0.35 towards one side.--Due to this c.m. motion, in the previous run the two independent 45⁰ roads were at different rapidities and a rapidity dependence of the cross sections was found.

4. INELASTIC INTERACTIONS AND COMPARISON WITH pd AND dd

Enough data have been collected with a minimum bias trigger for normal inelastic interactions. Half a million of events are on tapes for αp and αα interactions, more than could possibly be reconstructed due to limitations of available computer time, so we do not need to accumulate more minimum bias events.

A comparison of the inclusive distribution of particles in αα and αp interactions with the one in pp interactions is one of the major goals. Fig.6 shows the particle densities in αp and αα inelastic events normalized to the one in pp events as function of the rapidity for negative and positive tracks separately. The dramatic increase of the ratio for negative tracks at high rapidities at the α side and other features of the ratios can be, in part at least, qualitatively explained by the different quark composition of α's and p's. In order to account quantitatively for such effects a measurement with neutron or average-nucleon beams is needed.

Clearly, short runs with pd and dd beams after(!) an α run would be very valuable and could be justified for other reasons, too. For instance, dd collisions would provide an excellent comparison to $\alpha\alpha$ collisions (for the large p_t studies as well), since quark composition, average energy per nucleon and the field of the SFM and hence the acceptance, are all the same.

5. SPECTATOR PHYSICS

The SFM detector has the unique feature, that the spectrometer magnetic field is normal to the beam axis. Because of this, nuclear spectators (n, p, t and ^{3}He) that emerge at an angle close to 0^0 from the reaction are swept out of the beam pipe since their rigidity is different from that of the beam. Thus, the protons and ^{3}He are bent out one side of the beam pipe and the t and neutrons come out at the opposite side. We would like to tag these spectators (associated with events detected in the SFM detector) by species (p vs n, ^{3}He vs t), energy and p_t, by adding more MWPCs and a calorimeter in each magnet. The neutron calorimeter would be placed in the latter half of the compensator magnets on the neutron 0 degree side of the beam pipe. Because of the space limitations in the compensator magnet the dimensions of the calorimeter will be 4 collision lenghths in height, 7 collision lenghts in width, and 5 collision lengths thick. It will follow a similar design to the high density projection chamber design of O.Ullaland and H.G.Fischer. This will provide high resolution pattern recognition capability and some compensation for the nonuniform response of the calorimeter. Our goal for resolution in the center of the calorimeter is 30%, allowing discrimination between 1, 2 and 3 spectator nucleons.

In order to improve our track reconstruction capabilities at small angles, we plan to add more MWPCs. In particular, this will enhance the detection efficiency for spectators near the beam pipe.

The calorimeters are to be constructed at LBL. Final design decisions are being made now.

Contactperson: M.A. Faessler

References

[1] M.G.Albrow and M.Jacob (eds.),Physics with α particles, Discussion Meetings between Experimentalists and Theorists on ISR and Collider Physics (CERN, Geneva), Series 2, No.2 (Jan. 1981).

[2] M.A.Faessler, preprint CERN-EP/81-74 (Jul.1981), to be published in Nucl.Phys.A

[3] J.Berger et al., Nucl.Phys.A 338 (1980),421.

[4] A.Bujak et al.,Phys.Rev. D 23 (1981) 1895.

[5] M.G.Albrow and M.Jacob (eds.),Physics with α particles, Discussion Meetings between Experimentalists and Theorists on ISR and Collider Physics (CERN, Geneva), Series 2, No.3 (Feb. 1981).

[6] W.Bell et al.,(CERN-Heidelberg-Lund Coll.), paper in preparation.

[7] A.Karabarbounis et al., CERN-EP/81-46 (May 81) subm. to Phys.Lett..

[8] A.L.S.Angelis et al., 'High p_t π^0 Production with αα and αp Beams at the CERN ISR' submitted to the 20th Int. Conf. on High Energy Physics, Lisbon, 9-15 July 1981.

[9] J.W.Cronin et al., Phys.Rev.D11 (1975) 3105;
L.Kluberg et al., Phys.Rev.Lett.38 (1977) 670. D.Antreasyan et al., Phys.Rev.D19 (1979) 764.

[10] J.Pumplin and E.Yen, Phys.Rev.D11 (1975) 1812;
P.M.Fishbane and J.S.Trefil, Phys.Rev.D12 (1976) 2113;
J.H.Kuhn, Phys.Rev.D13 (1976) 2948;
P.M.Fishbane et al., Phys.Rev.D16 (1977) 122;
A.Krzywicki et al., Phys.Lett. 85B (1979) 407.

[11] B.Alper et al., Nucl.Phys.B100 (1975) 237.

[12] SFM unpublished data (ACCDW collaboration).

[13] C.R.Gruhn CERN/EF 81-9.

Figure Captions for fig.2 and fig.3

Fig.2 Invariant cross-sections $d^2\sigma/\pi dyd(p^2_t)$ in units of μb $GeV^{-2}c^3$ as function of p_t. The lines through the points correspond to the fitted exponential slope (see text and table 1). The cross sections are compared with pp data (lower points) from ref.[9] (CP,$\sqrt{s}$=27GeV, y=0) and ref.[11] (BS,$\sqrt{s}$=31 and 44 GeV,y_{cm}=0.,0.6 and 1.) and with pp cross sections times 4 (a,b) or times 16 (c,d) (shaded areas)

a) pα collisions, positive tracks.

b) pα collisions, negative tracks.

c) αα collisions, positive tracks.

d) αα collisions, negative tracks.

Fig.3 The ratios of invariant cross-sections in αp and αα collisions to the ones in pp collisions as function of p_t:

a) pα collisions, positive tracks, y_{cm} = -0.48±.25

b) pα collisions, negative tracks, y_{cm} = -0.28±.25

Circles: pp data [11] ($\sqrt{s}$ = 44 GeV, y= 0 - 1)

Crosses : pp data [12] ($\sqrt{s}$=63 GeV) extrapolated to 44 GeV

Solid lines : $R = 4^{a(p_t)}$ with $\alpha^+(p_t)$ from ref.[ ]

c) αα collisions, positive tracks, ycm =.83±.25.

d) αα collisions, negative tracks, ycm= .63±.25.

Circles: pp data from ref.[11] ($\sqrt{s}$=31 GeV, y=0.)

Triangles: pp data from ref.[11] ($\sqrt{s}$=31 GeV, y=0.6)

Crosses: pp data from ref.[12] ($\sqrt{s}$=63GeV) extrapolated to 31GeV

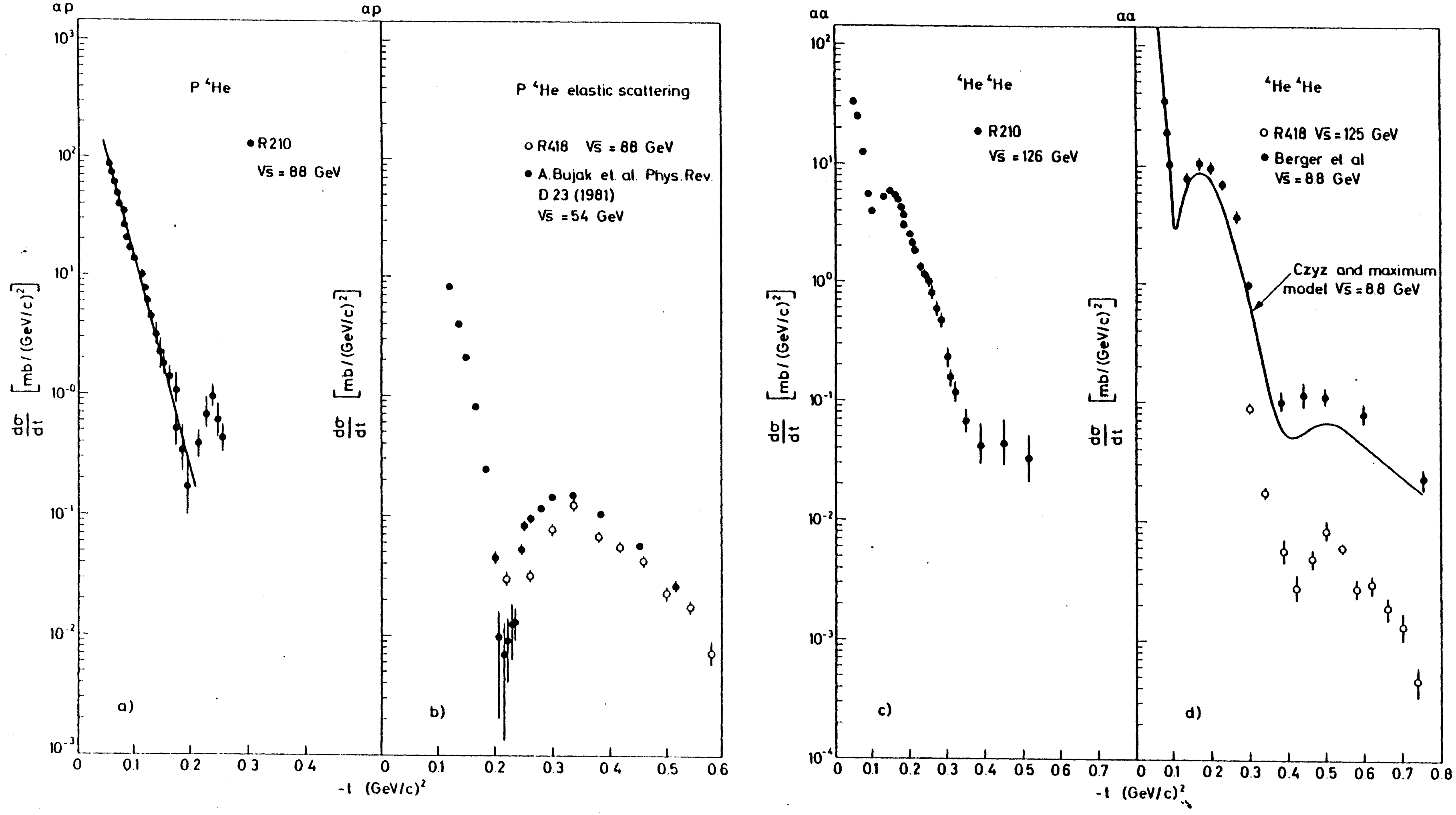

Fig.1 Differential elastic cross-sections $d\sigma/dt$ versus $|t|$ ($|t| \approx s \cdot \sin^2 \theta_{cm}/2$). Preliminary data:

a) αp; experiments R210/211 ($\sqrt{s}$ = 88 GeV) (Ref. 4)

b) αp; experiments R418 ($\sqrt{s}$ = 88 GeV) compared with Ref. ~~5~~ 4 ($\sqrt{s}$ = 54 GeV)

c) αα; experiments R210/211 ($\sqrt{s}$ = 125 GeV)

d) αα; experiment R418 ($\sqrt{s}$ = 125 GeV) compared with Ref. ~~6~~ 3 ($\sqrt{s}$ = 8.8 GeV)

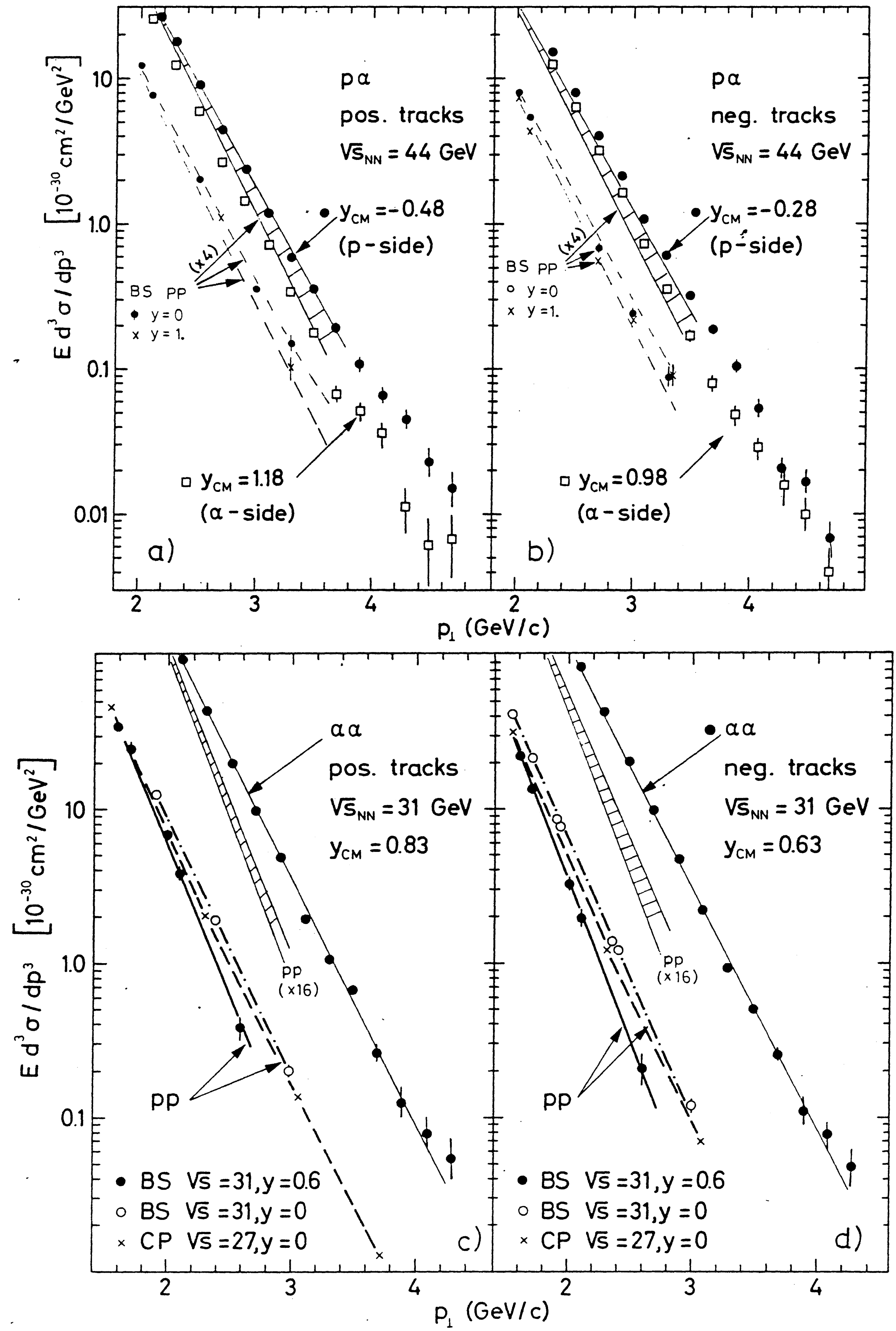
pα
pos. tracks
√s_NN = 44 GeV
y_CM = -0.48
(p-side)
y_CM = 1.18
(α-side)
BS pp
y = 0
y = 1.
(x4)
a)
pα
neg. tracks
√s_NN = 44 GeV
y_CM = -0.28
(p-side)
y_CM = 0.98
(α-side)
BS pp
y = 0
y = 1.
(x4)
b)
p⊥ (GeV/c)
E d³σ/dp³ [10⁻³⁰ cm²/GeV²]
αα
pos. tracks
√s_NN = 31 GeV
y_CM = 0.83
pp
(x16)
pp
BS √s = 31, y = 0.6
BS √s = 31, y = 0
CP √s = 27, y = 0
c)
αα
neg. tracks
√s_NN = 31 GeV
y_CM = 0.63
pp
(x16)
pp
BS √s = 31, y = 0.6
BS √s = 31, y = 0
CP √s = 27, y = 0
d)
p⊥ (GeV/c)
E d³σ/dp³ [10⁻³⁰ cm²/GeV²]

Fig.2

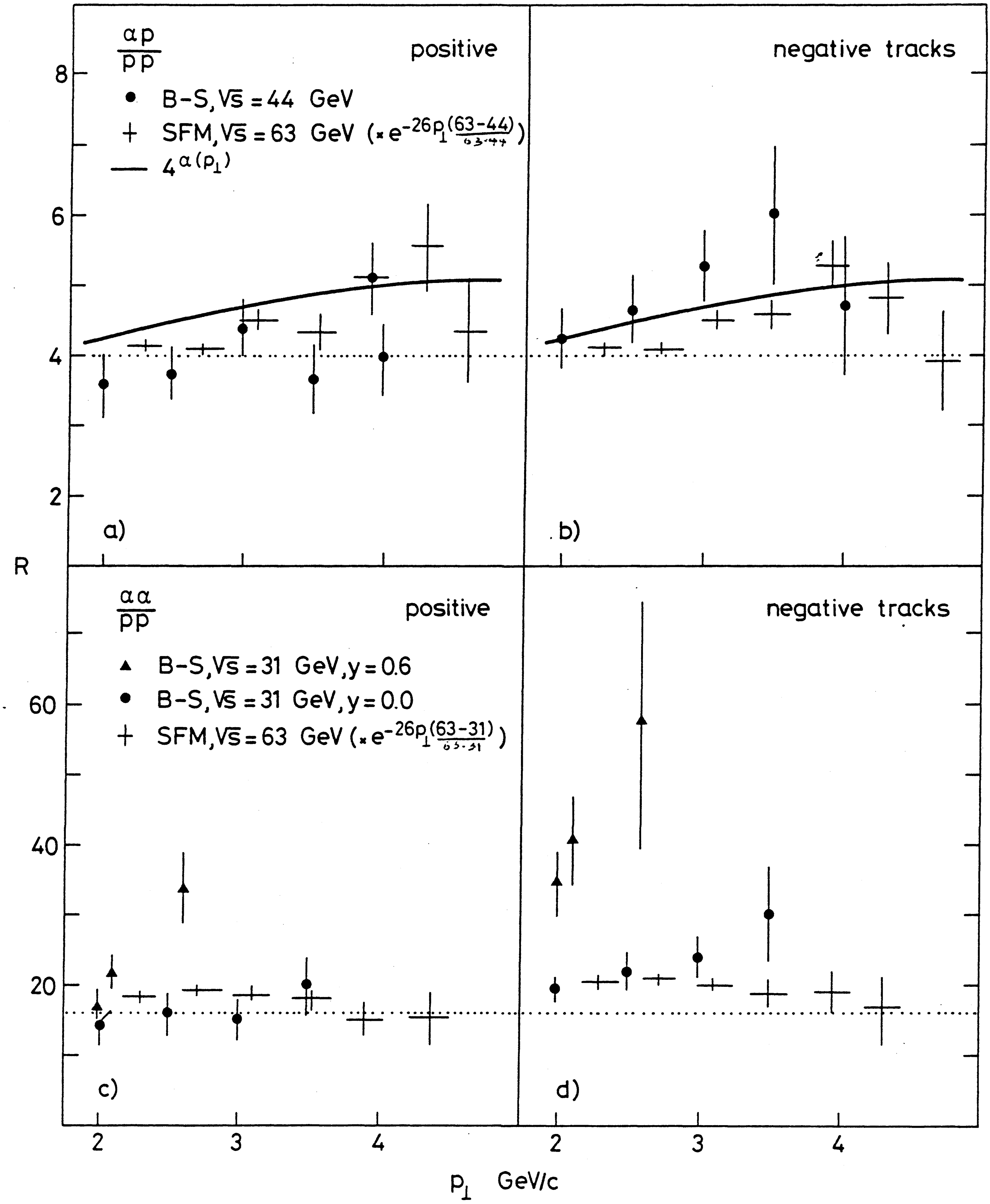

αp / pp
positive
negative tracks
B-S, √s = 44 GeV
SFM, √s = 63 GeV (× e^-26p⊥(63-44)/(63·44))
— 4^α(p⊥)
a)
b)
R
αα / pp
positive
negative tracks
B-S, √s = 31 GeV, y = 0.6
B-S, √s = 31 GeV, y = 0.0
SFM, √s = 63 GeV (× e^-26p⊥(63-31)/(63·31))
c)
d)
p⊥ GeV/c

Fig.3

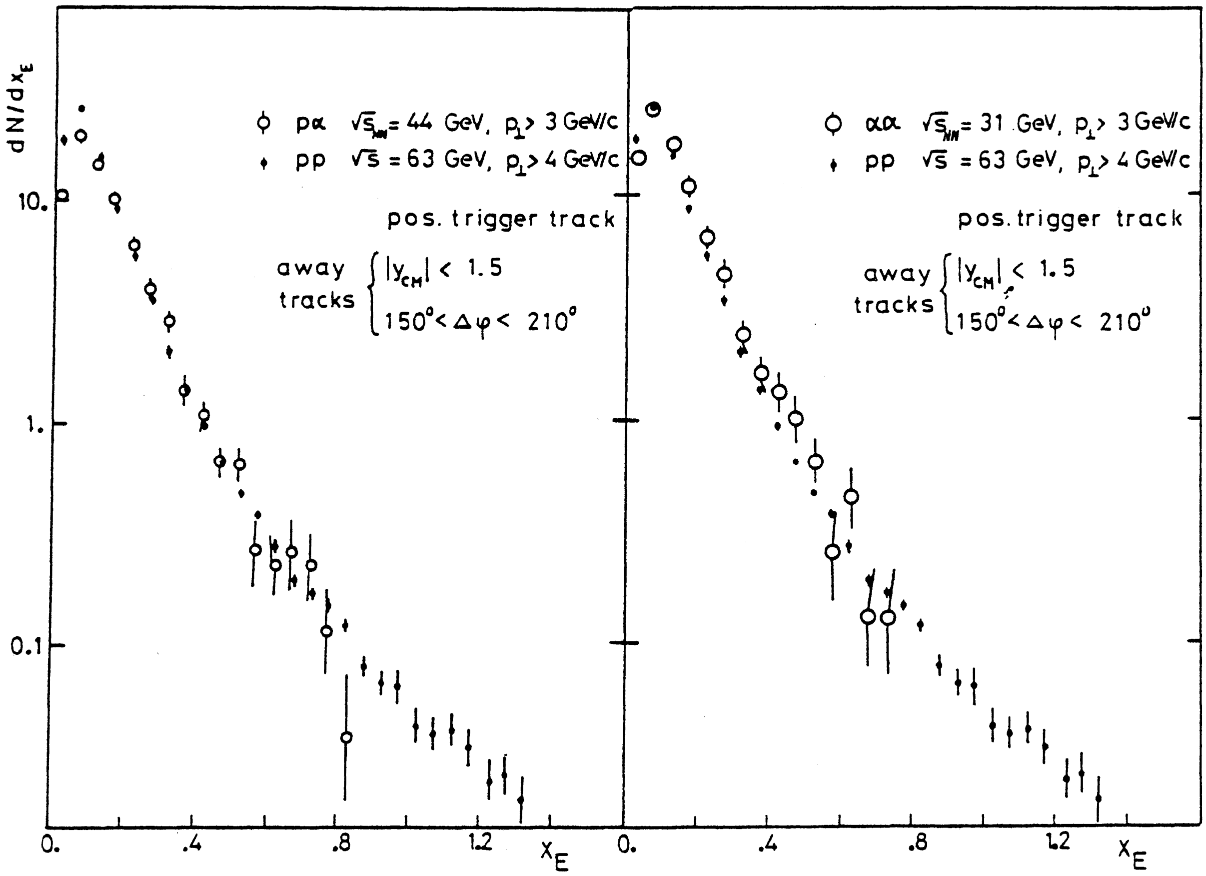

Fig.4 The distribution dN/dx_E of particles opposite to a positive large p_T trigger track ($150° < \Delta\phi < 210°$ and $|y_{cm}| < 1.5$) for
a) αp collisions (p_T of trigger > 3 GeV/c)
b) $\alpha\alpha$ collisions with a positive trigger (p_T of trigger > 3 GeV/c)
compared with the one for pp collisions (p_T of trigger > 4 GeV/c).

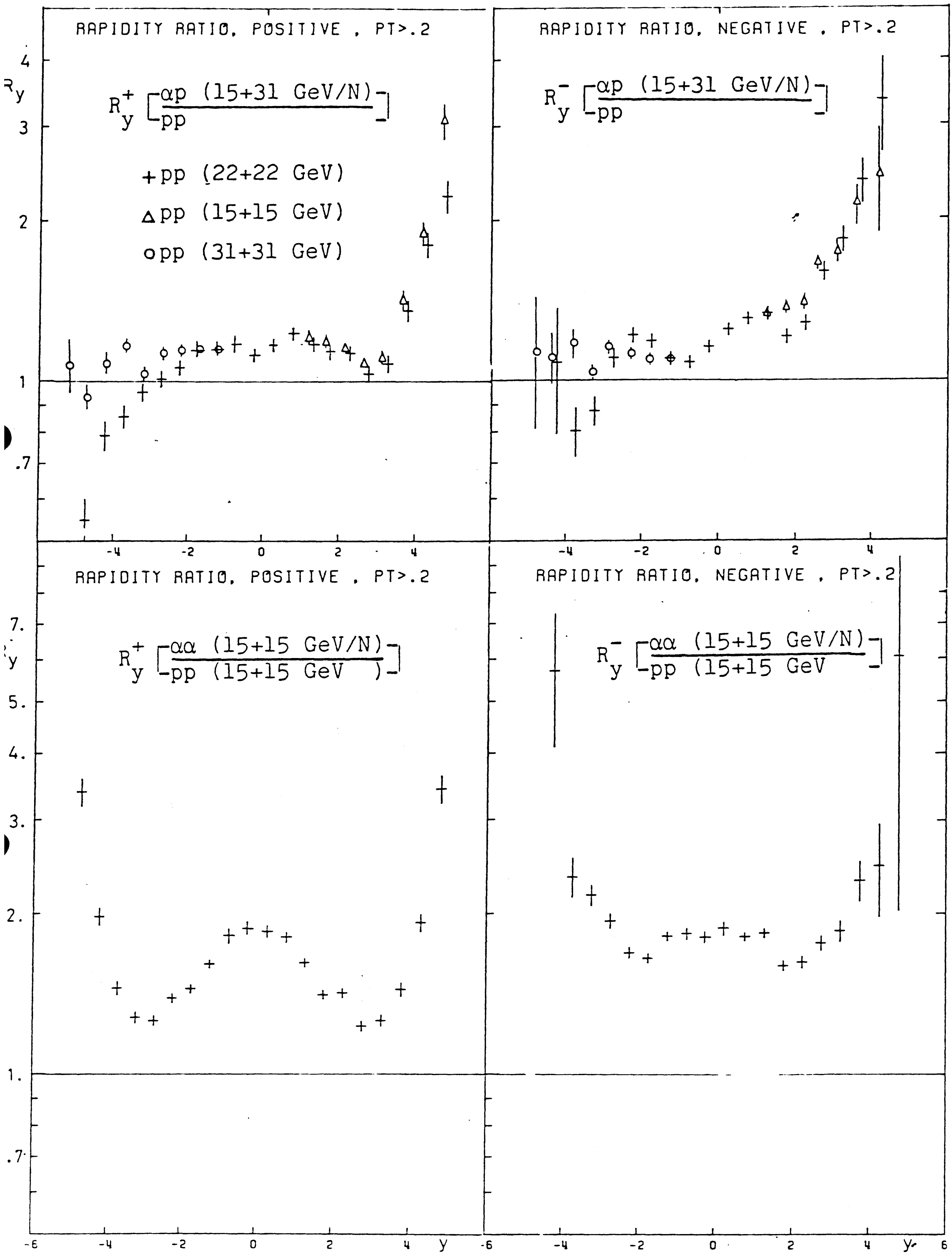

Fig.5 Ratios of particle densities as a function of the rapidity $y_{cm} = \frac{1}{2} \ln(E+p_L)/(E-p_L)$ a) $R_y^+(\alpha p/pp)$, b) $R_y^-(\alpha p/pp)$, c) $R_y^+(\alpha\alpha/pp)$, d) $R_y^-(\alpha\alpha/pp)$.